



## Preparation of Surface Imprinted Magnetic Nanoparticles for Selective Detection of Ciprofloxacin in Milk

Adem ZENGİN<sup>1,\*</sup><sup>1</sup>Van Yuzuncu Yil University, Faculty of Engineering, Department of Chemical Engineering, 65080 Tuşba, Van, Turkey

### Article Info

Received: 22/04/2017

Accepted: 21/09/2017

### Keywords

*magnetic nanoparticles  
molecularly imprinting  
magnetic separation  
ciprofloxacin  
milk*

### Abstract

Molecularly imprinted polymers were synthesized for selective detection of ciprofloxacin on magnetic nanoparticles via surface-initiated free radical polymerization. Methacrylic acid, ethylene glycol dimethacrylate, azobisisobutyronitrile and ciprofloxacin were used for the formation of molecularly imprinted layer as a functional monomer, cross linker, initiator and template molecule, respectively. The surface characterization of the prepared nanoparticles was carried out by using several methods such as TEM, XPS and VSM. The prepared imprinted nanoparticles had high binding capacity and fast adsorption kinetics. Additionally, the prepared nanoparticles showed superparamagnetic property with rapid magnetic separation and retained binding selectivity after ten adsorption-desorption cycles. The imprinted magnetic nanoparticles were subsequently applied for selective separation and determination of CPX from milk with high recoveries (98.0% - 98.8%) and low relative standard deviations (2.76% - 4.59%). All the results have shown that the developed new method is a good alternative for the selective separation of ciprofloxacin in complex medium.

## 1. INTRODUCTION

Ciprofloxacin, a fluoroquinolone derivative antibiotic, is frequently used in the treatment of diseases caused by Gram-negative and Gram-positive bacteria through inhibiting DNA gyrase enzyme which is an important enzyme in bacterial DNA replication [1,2]. The pharmacokinetic properties of CPX are characterized by good absorption and wide distribution in various animal fluids and tissues. However, controlling the concentration and residues of such antibiotics is very important not only to examine their pharmacokinetic properties but also to synthesize and develop new type of antibiotics [3-5]. CPX antibiotic is frequently used in veterinary medicine so there is a possibility of presence of CPX in animal-derived foods. The presence of such antibiotics in animal fluids/tissues and the consumption of these animal foods by human pose a serious threat to human health. In addition, bacteria become more resistant to these drugs because of the excessive using of CPX antibiotics which may lead to more serious consequences for human. For this reason, CPX determination in animal-derived foods such as milk, eggs and meat is very important task in terms of public health. Several analytical methods have been reported for the determination of CPX in biological fluids and tissues such as voltammetry [6], liquid chromatography [7], immunosorbent assay [8], spectrophotometric method [9], and capillary electrophoresis [10]. Most of these methods have some merits such as complicated secondary extraction step (liquid-liquid extraction or solid-liquid extraction), using of large amounts of solvents and time-consuming. Moreover, the selectivity of these methods is low due to complex nature of the biological fluids or tissues.

Molecularly imprinting is a synthetic method for preparation of polymer materials which has pre-designed molecular recognition ability. Due to this feature, molecularly imprinted materials are often named as plastic antibody or enzyme mimics [11]. Molecularly imprinted polymers (MIPs) can be used to

\*Corresponding author, e-mail: ademzengin@yyu.edu.tr

design functional polymeric materials with selective recognition properties. After polymerization with a suitable monomer and template molecule, the template molecule is removed from the polymer matrix to form three-dimensional cavities in the polymer matrix that are the same size, shape and functionality as compared with the template molecule. Molecularly imprinted polymers have several advantages over their biological counterparts: low cost, easy to prepare, high stability, high mechanical strength, and applicable in most chemical environments. Thanks to these features, molecularly imprinted materials are frequently used in biosensors, catalysis and many other applications [12].

Magnetic nanoparticles have a wide range of applications such as magnetic fluids, catalysis, biotechnology, biological imaging [13-16]. Magnetic nanoparticles can be synthesized in different shapes and phases such as iron oxides such ( $\text{Fe}_3\text{O}_4$  and  $\text{Fe}_2\text{O}_3$ ), pure metals (Fe, Co), spinel type ferromagnets ( $\text{MgFe}_2\text{O}_4$ ,  $\text{MnFe}_2\text{O}_4$  and  $\text{CoFe}_2\text{O}_4$ ), and alloys ( $\text{CoPt}_3$  and  $\text{FePt}$ ) [17-21]. Among such particles, superparamagnetic nanoparticles are more preferred as an adsorbent for rapid and simple removal of the target molecule from the sample matrix. Thanks to superparamagnetism, the particles are collected very easily by the applied external magnetic field via a simple magnet and redispersed easily when the magnetic field is removed. Despite these advantages, superparamagnetic nanoparticles have some drawbacks: (i) low molecular selectivity; (ii) low adsorption capacity; (iii) self-aggregation due to high surface area/volume ratio; (iv) decreasing of superparamagnetic property when in contact with air. The synthesis of molecularly imprinted polymers on magnetic nanoparticles not only preserves the superparamagnetic property of the particles but also overcomes the above disadvantages [22,23].

In the present work, a novel superparamagnetic CPX imprinted  $\text{Fe}_3\text{O}_4$  nanoparticle ( $\text{Fe}_3\text{O}_4\text{@MIP}$ ) was synthesized via surface-initiated free radical polymerization. The  $\text{Fe}_3\text{O}_4$  nanoparticles were first functionalized with a methacrylate group containing organosilane and then polymerization was performed in the presence ciprofloxacin (template molecule, CPX), methacrylic acid (MAA, functional monomer), ethylene glycol dimethacrylate (EGDMA, cross-linker), azobisisobutyronitrile (AIBN, initiator) and acetonitrile (solvent or porogen). The prepared  $\text{Fe}_3\text{O}_4\text{@MIP}$  nanoparticles were characterized by several surface characterization methods such as transmission electron microscopy (TEM), X-ray photoelectron spectroscopy (XPS), vibrating sample magnetometer (VSM). The binding properties of the prepared  $\text{Fe}_3\text{O}_4\text{@MIP}$  nanoparticles were further studied by equilibrium properties, binding capacity and selectivity experiments. Moreover, the usability of the prepared  $\text{Fe}_3\text{O}_4\text{@MIP}$  nanoparticles was further assessed for removal and enrichment of CPX from milk.

## 2. EXPERIMENTAL

### 2.1. Materials and Reagents

$\text{FeCl}_3 \cdot 6\text{H}_2\text{O}$ ,  $\text{FeCl}_2 \cdot 4\text{H}_2\text{O}$ ,  $\text{NH}_4\text{OH}$  solution (28%), 3-(trimethoxysilyl) propyl methacrylate (MPS), methacrylic acid (MAA), ethylene glycol dimethacrylate (EGDMA), methanol, acetonitrile, and acetic acid were purchased from Sigma-Aldrich at available highest purity and used as received unless otherwise stated. Azobis(isobutyronitrile) (AIBN, Across 98%) was recrystallized in ethanol. Ciprofloxacin (CPX), Ciprofloxacin lactate (CPFL), and moxifloxacin (MPX) were purchased from Bayer (Germany) and used without any purification. Double distilled deionized water was used in all experiments.

### 2.2. Instrumentation

The morphology and structure analysis of the prepared nanoparticles were investigated by transmission electron microscopy (TEM, JEOL 1400). 5  $\mu\text{L}$  of the nanoparticle dispersion was dropped on the carbon coated copper grid and left to dry at room temperature. X-ray photoelectron spectroscopy (XPS) analysis was examined by a SPECS XPS spectrometer using Al  $K\alpha$  as an X-ray source. Magnetic properties of the prepared nanoparticles were characterized by vibrating sample magnetometer (VSM) from Cryogenic Limited PPMS system. UV-vis analysis was done with a Shimadzu UV-2550 spectrophotometer at room temperature.

### 2.3. Preparation of Fe<sub>3</sub>O<sub>4</sub> and Fe<sub>3</sub>O<sub>4</sub>@MPS Nanoparticles

Superparamagnetic Fe<sub>3</sub>O<sub>4</sub> nanoparticles were synthesized via chemical co-precipitation of Fe<sup>3+</sup> and Fe<sup>2+</sup> in the basic medium [24]. Briefly, FeCl<sub>3</sub>.6H<sub>2</sub>O and FeCl<sub>2</sub>.4H<sub>2</sub>O were dissolved in 50 mL of deionized water with a molar ratio of 0.5. 20 mL of NH<sub>4</sub>OH was added to the solution under nitrogen atmosphere and the formed black precipitate was vigorously stirred with a mechanical stirrer at 800 rpm for 30 min at room temperature. The mixture was additionally stirred for 30 min at 80 °C. The black precipitate was collected with an external magnet and washed with deionized water until the pH of the washing water reached to 7 and finally, the nanoparticles were dried under vacuum.

To prepare Fe<sub>3</sub>O<sub>4</sub>@MPS nanoparticles, 200 mg of the prepared Fe<sub>3</sub>O<sub>4</sub> nanoparticles was added to 200 mL of toluene and the mixture was ultrasonicated for 10 min at room temperature. Then, 500 µL of the MPS was added to the dispersion and the dispersion was stirred at 90 °C under nitrogen atmosphere (to prevent self-polymerization of MPS) for 8 hours. The MPS coated magnetic nanoparticles were collected via external magnet and sequentially rinsed with toluene, toluene:methanol (1:1, v/v) and methanol. The Fe<sub>3</sub>O<sub>4</sub>@MPS nanoparticles were dried under vacuum and stored in a vacuum desiccator until used.

### 2.4. Preparation of Fe<sub>3</sub>O<sub>4</sub>@MIP and Fe<sub>3</sub>O<sub>4</sub>@NIP Nanoparticles

50 mg of Fe<sub>3</sub>O<sub>4</sub>@MPS was dispersed in 50 mL of acetonitrile and then 18.1 mg MAA, 310 µL EGDMA, 7.2 mg AIBN and 78.5 mg CPX were added to this solution, sequentially. The mixture was purged with nitrogen for 15 min in an ice bath and subsequently, stirred on a temperature controlled shaker at 400 rpm at 60 °C for 16h. The resultant Fe<sub>3</sub>O<sub>4</sub>@MIP nanoparticles were collected by an external magnet and rinsed with acetonitrile and ethanol several times. The Fe<sub>3</sub>O<sub>4</sub>@NIP (non-imprinted nanoparticles) nanoparticles were prepared as the same method in the absence of CPX.

### 2.5. Determination of Binding Properties

Before determination of the binding properties of the Fe<sub>3</sub>O<sub>4</sub>@MIP nanoparticles, the template molecule, CPX was removed from the polymer layer by using methanol: acetic acid mixture (3:1, v/v). The prepared magnetic nanoparticles were dispersed in the methanol:acetic acid mixture and stirred in an orbital shaker at 300 rpm and the extraction solution was changed every three hours until the no template molecule was detected by UV-vis spectrophotometer at 326 nm. Subsequently, the magnetic nanoparticles were rinsed with acetic acid and methanol several times, respectively. The resultant magnetic nanoparticles were dried under vacuum.

To determine the static equilibrium properties, 3.0 mg of Fe<sub>3</sub>O<sub>4</sub>@MIP was mixed with different amounts of CPX solution (0.2-2.8 mg/mL) in 3.0 mL of acetonitrile in eppendorf tubes. The tubes were sealed and incubated on an orbital shaker for 1 h at room temperature. After incubation, the Fe<sub>3</sub>O<sub>4</sub>@MIP nanoparticles were collected by an external magnet and the concentration of the CPX in supernatants were determined by UV-vis spectrophotometer at 326 nm. The Same experimental protocol was applied to the Fe<sub>3</sub>O<sub>4</sub>@NIP nanoparticles.

The equilibrium concentration of the CPX was estimated according to the equation given below:

$$Q = (C_i - C_f) \frac{V}{m}$$

where Q (mg/g) is the equilibrium concentration of CPX, C<sub>i</sub> (mg/mL) is the initial concentration of CPX, C<sub>f</sub> (mg/mL) is the final concentration of CPX after incubation, V (mL) is the total volume of the mixture, and m (mg) is the mass of the magnetic nanoparticles.

3.0 mg of Fe<sub>3</sub>O<sub>4</sub>@MIP was dispersed in CPX solution (2.2 mg/mL in 3.0 mL acetonitrile) and incubated for different time intervals (5-90 min) on an orbital shaker at room temperature for the adsorption experiments. After incubation, Fe<sub>3</sub>O<sub>4</sub>@MIP nanoparticles were collected and the CPX concentration of supernatant was determined by UV-vis spectrophotometer at 326 nm. Same experimental protocol was applied to the Fe<sub>3</sub>O<sub>4</sub>@NIP nanoparticles.

CPFL and MPX were selected as structural analogues of CPX for the selectivity experiments. 3.0 mg of Fe<sub>3</sub>O<sub>4</sub>@MIP nanoparticle was dispersed in the solutions of CPX and its analogues (2.2 mg/mL in 3.0 mL acetonitrile) for 1 h at room temperature. After incubation, the magnetic nanoparticles were collected and the concentration of each compound in supernatant was determined by UV-vis spectrophotometer. Same experimental protocol was applied to the Fe<sub>3</sub>O<sub>4</sub>@NIP nanoparticles.

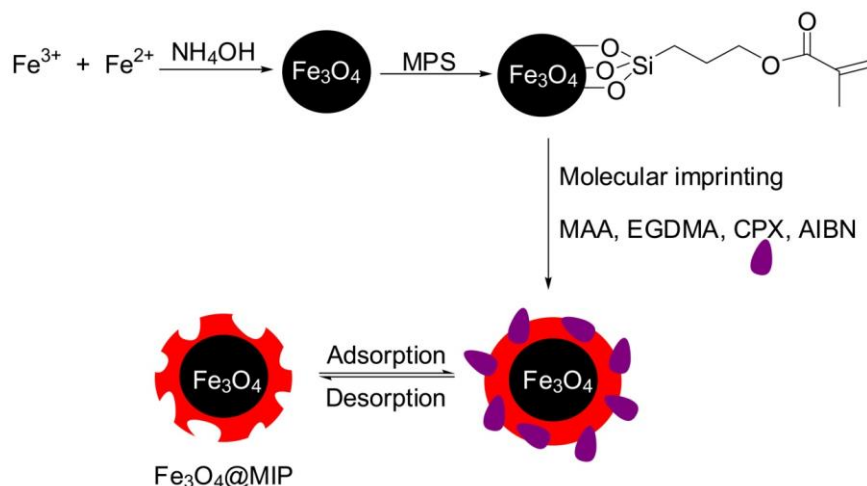
## 2.6. Determination of CPX in Milk

The milk sample was purchased from local grocery market. Firstly, the milk sample was filtered through a sterile millipore membrane (pore diameter: 0.2 μm) [25] and diluted ten times with phosphate buffer solution (0.1 M, pH 7.4). The diluted milk samples (5 mL) were homogenized by vortex mixing for 5 min. Then, the homogenized milk samples were spiked with different CPX solutions, making the final concentrations 2.0 μg/L, 4.0 μg/mL, 6.0 μg/L, 8.0 μg/L. The Fe<sub>3</sub>O<sub>4</sub>@MIP nanoparticles (5.0 mg) were added to the spiked milk samples and incubated for 1 h at room temperature. After incubation, the Fe<sub>3</sub>O<sub>4</sub>@MIP nanoparticles were collected and the concentration of CPX in supernatant was determined by UV-vis spectrophotometer at 326 nm (see Supplementary Material Figure S1 for UV-vis spectra of spiked and unspiked milk samples). Same experimental protocol was applied to the Fe<sub>3</sub>O<sub>4</sub>@NIP nanoparticles.

## 3. RESULTS AND DISCUSSION

### 3.1. Characterization of Fe<sub>3</sub>O<sub>4</sub>@MIP and Fe<sub>3</sub>O<sub>4</sub>@NIP Nanoparticles

Surface imprinting is a very useful method for preparing molecularly imprinted polymers on or near the particle surface, allowing mass transfer. Scheme 1 illustrated the three main steps for the preparation of molecularly imprinted nanoparticles. In the first step, Fe<sub>3</sub>O<sub>4</sub> nanoparticles were synthesized by coprecipitation of iron ions in basic medium. After preparation of the magnetic nanoparticles, methacrylate terminated nanoparticles were prepared by chemical modification with MPS molecules on the magnetic nanoparticles for initiating polymerization. Afterwards, the methacrylate terminated nanoparticles were dispersed in ACN solution containing MAA, EGDMA, and CPX. A uniform molecularly imprinted polymer layer was formed on the magnetic nanoparticles after polymerization. In the last step, the recognition cavities were formed after removal of the template molecule on or near the surface of the imprinted polymeric layer.



**Scheme 1.** Schematic representation of the preparation of Fe<sub>3</sub>O<sub>4</sub>@MIP nanoparticles.

The chemical composition of the nanoparticles after each step was examined by XPS analysis. The wide scan XPS spectrum of the nanoparticles and relative atomic concentration of the nanoparticles were given in Figure 1 and Table 1, respectively. The pristine magnetic nanoparticles (Figure 1a) showed four main peaks located at 711 eV, 720 eV, 529 eV and 285 eV corresponding to Fe 2p<sub>3/2</sub>, Fe 2p<sub>1/2</sub>, O 1s and C 1s, respectively. The presence of the C element (3.9 % atomic concentration) for the bare magnetic nanoparticles indicated that some contamination occurred during XPS operation [26]. The increase of the O 1s and C 1s intensities and relative atomic concentrations for oxygen and carbon after incorporation of the MPS molecule on the magnetic nanoparticles was indicated that chemical attachment of the MPS groups successfully occurred (Figure 1b and Table 1). In addition, core-level XPS spectra of MPS modified magnetic nanoparticles consists of Fe 2p, O 1s and C 1s peaks curve fitted to components with binding energies of 710.1 eV (Fe 2p<sub>1/2</sub>) and 723.3 eV (Fe 2p<sub>3/2</sub>) for Fe 2p, 530.7 eV (C=O) and 531.3 eV (C-O) for O 1s, 285.0 eV (C-C/C-H), 285.8 eV (C-O) and 290.0 eV (O-C=O) for C 1s (Supplementary Material, Figure S2). The decrease in iron peak intensity and the increase in carbon and oxygen peak intensities after molecular imprinting was the strongest evidence of the formation of a polymer layer on the nanoparticle surfaces (Figure 1c). Moreover, increasing atomic concentration of oxygen/carbon, and decreasing of atomic concentration of iron elements additional evidence of the presence of a polymer layer on the nanoparticles (Table 1). However, the fact that the iron peaks could still be detected indicating that the polymer layer thickness on the particle surface is less than 10 nm which is typical depth length of X-rays.

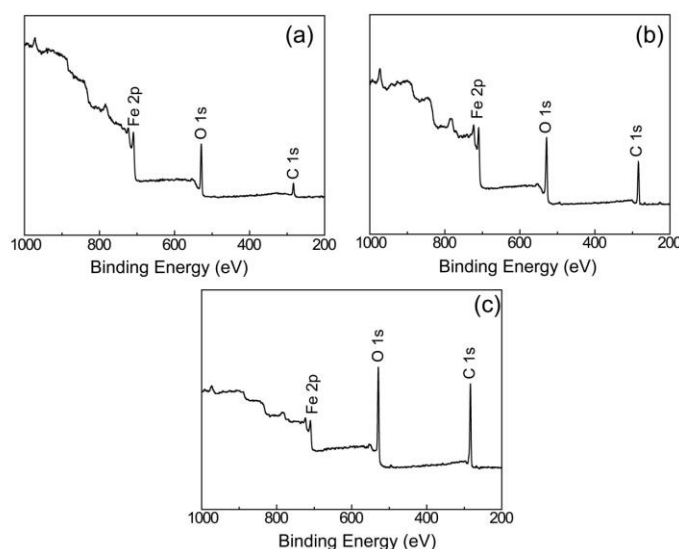


**Figure 1.** XPS wide spectrum of  $Fe_3O_4$  (a),  $Fe_3O_4@MPS$  (b),  $Fe_3O_4@MIP$  (c).

**Table 1.** Relative atomic concentration of the prepared nanoparticles determined by XPS.

Sample	Elements, %		
	Fe	O	C
$Fe_3O_4$	41.2	54.9	3.9
$Fe_3O_4@MPS$	19.5	57.2	23.3
$Fe_3O_4@MIP$	4.1	60.5	35.4

The morphology and diameters of each nanoparticle were determined by TEM analysis. TEM images of each particle were given in Figure 2. The pristine and MPS-functionalized magnetic nanoparticles were agglomerated (this was expected due to high magnetization properties of the nanoparticles) and mean diameters were 12 nm (Figure 2a and Figure 2b). After polymerization, it was clearly seen that similar morphologies were obtained and a polymeric layer was formed on the MPS coated magnetic nanoparticles for  $Fe_3O_4@MIP$  and  $Fe_3O_4@NIP$  nanoparticles (Figure 2c and Figure 2d). The average

thickness of the polymer layer was calculated to be 6 nm for both nanoparticles. The agglomeration of nanoparticles was still present due to most probably the polymeric layer on the particle surface restricted the movement of the particles to form an eccentric structure [27].

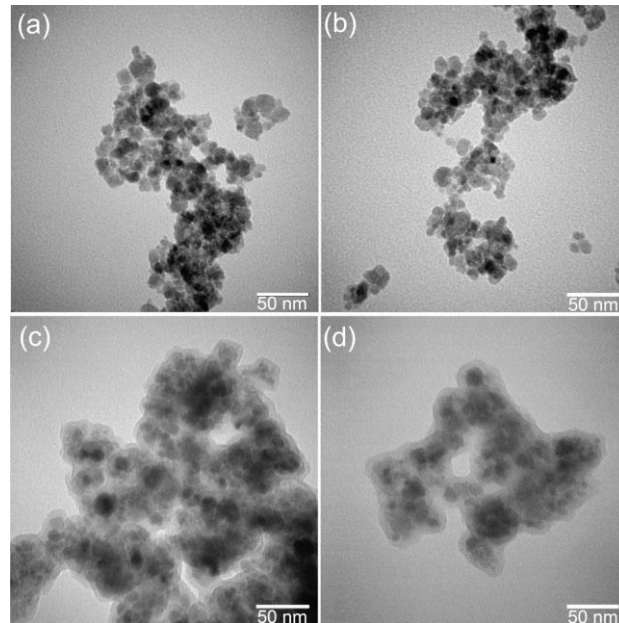


**Figure 2.** TEM images of  $Fe_3O_4$  (a),  $Fe_3O_4@MPS$  (b),  $Fe_3O_4@MIP$  (c).

Magnetic properties of  $Fe_3O_4$ ,  $Fe_3O_4@MPS$  and  $Fe_3O_4@MIP$  nanoparticles were studied by VSM at room temperature and magnetic hysteresis loops of the nanoparticles were shown in Figure 3. The saturation magnetization value of the  $Fe_3O_4$  nanoparticles was found to be 63.2 emu/g (Figure 3a). The saturation magnetization value of the  $Fe_3O_4@MPS$  decreased to 58.3 emu/g (Figure 3b). The slight decrease in the magnetization value was due to the formation of monolayer of the MPS molecule on the  $Fe_3O_4$  nanoparticles. After polymerization, the saturation magnetization value of the  $Fe_3O_4@MIP$  nanoparticles was drastically decreased to 39.1 emu/g (Figure 3c) because of the presence of a polymer layer as observed by TEM (Figure 2c.). In all cases, the magnetic hysteresis loops also showed no remanence or coercivity indicating that all prepared magnetic nanoparticles had superparamagnetic behavior at room temperature. The  $Fe_3O_4@MIP$  particles could be collected very easily for a short time period (~ 40 s) via an external magnet at room temperature because of their superparamagnetic properties (Figure 3 inset). This is so important for magnetic separation of interested molecules in complex media such as urine, serum, milk, etc.

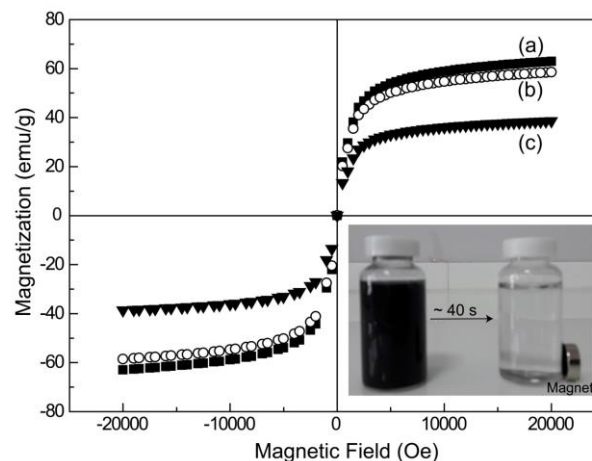


**Figure 3.** VSM curves of  $Fe_3O_4$  (a),  $Fe_3O_4@MPS$  (b),  $Fe_3O_4@MIP$  (c).

### 3.2. Adsorption Capacity of Fe<sub>3</sub>O<sub>4</sub>@MIP and Fe<sub>3</sub>O<sub>4</sub>@NIP Nanoparticles

The static adsorption experiments were carried out to determine the adsorption capacity of the Fe<sub>3</sub>O<sub>4</sub>@MIP and Fe<sub>3</sub>O<sub>4</sub>@NIP nanoparticles by using different initial concentration of CPX for adsorption time of 60 min at room temperature. As shown in Figure 4, the adsorption capacity of Fe<sub>3</sub>O<sub>4</sub>@MIP and Fe<sub>3</sub>O<sub>4</sub>@NIP nanoparticles increased as the initial concentration of CPX increased. When the initial concentration of CPX was 2.2 mg/mL, the adsorption capacity reached to 31.1 mg/g and 9.7 mg/g for of Fe<sub>3</sub>O<sub>4</sub>@MIP and Fe<sub>3</sub>O<sub>4</sub>@NIP, respectively. The adsorption capacity did not change for high initial concentration of CPX for both nanoparticles. It was obviously seen that the Fe<sub>3</sub>O<sub>4</sub>@MIP nanoparticles had specific binding cavities to the template molecule of CPX than Fe<sub>3</sub>O<sub>4</sub>@NIP nanoparticles.

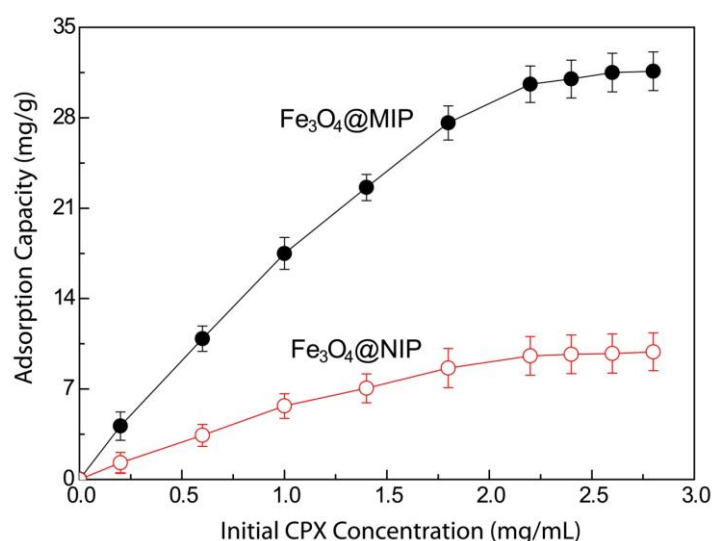


**Figure 4.** Adsorption isotherms of CPX on the Fe<sub>3</sub>O<sub>4</sub>@MIP and Fe<sub>3</sub>O<sub>4</sub>@NIP nanoparticles (Adsorption conditions: 1.0 mg/mL nanoparticle, 2.2 mg/mL initial concentration of CPX, T = 25 °C).

Scatchard analysis [28] was employed to the data obtained from the static adsorption experiments to demonstrate the quantitatively the binding properties of the imprinted and non-imprinted nanoparticles. Scatchard equation is expressed as given below:

$$\frac{Q}{C_e} = \frac{Q_{\max}}{K_d} - \frac{Q}{K_d}$$

where Q (mg/g) is the amount of CPX bound to the Fe<sub>3</sub>O<sub>4</sub>@MIP and Fe<sub>3</sub>O<sub>4</sub>@NIP at equilibrium, Q<sub>max</sub> (mg/g) is the theoretical maximum adsorption capacity, C<sub>e</sub> (mg/mL) is the free analytical concentration of CPX at equilibrium and K<sub>d</sub> (mg/mL) is the dissociation constant. The values of K<sub>d</sub> and the Q<sub>max</sub> can be estimated from slope and intercept of the linear plotted in Q/C<sub>e</sub> versus Q. The theoretical maximum adsorption capacity of Fe<sub>3</sub>O<sub>4</sub>@MIP for CPX was 37.8 mg/g with a dissociation constant 0.411 and the theoretical maximum adsorption capacity of Fe<sub>3</sub>O<sub>4</sub>@NIP for CPX was 11.8 mg/g with a dissociation constant 0.227. The results also approved that the Fe<sub>3</sub>O<sub>4</sub>@MIP nanoparticles had much stronger recognition ability toward CPX than the Fe<sub>3</sub>O<sub>4</sub>@NIP nanoparticles.

### 3.3. Adsorption Kinetics of Fe<sub>3</sub>O<sub>4</sub>@MIP and Fe<sub>3</sub>O<sub>4</sub>@NIP Nanoparticles

The adsorption kinetic of molecularly imprinted nanoparticles is a very important parameter in many applications. The adsorption kinetics of the Fe<sub>3</sub>O<sub>4</sub>@MIP and Fe<sub>3</sub>O<sub>4</sub>@NIP nanoparticles were investigated by using an initial concentration of 2.2 mg/mL by different adsorption time intervals (5-90 min) and the results were shown in Figure 5. The adsorption capacity of the Fe<sub>3</sub>O<sub>4</sub>@MIP nanoparticles was rapidly increased to 28.9 mg/g within 30 min and slightly increased to 31.6 mg/g after additional 15 min. After

prolonged adsorption time, the adsorption capacity did not change and reached a plateau value at constant adsorption capacity. The adsorption capacity of  $\text{Fe}_3\text{O}_4\text{@NIP}$  was also studied. The adsorption capacity of CPX on the  $\text{Fe}_3\text{O}_4\text{@NIP}$  nanoparticles was very low and at prolonged adsorption time, the adsorption capacity was kept at 9.9 mg/g indicated that the  $\text{Fe}_3\text{O}_4\text{@MIP}$  nanoparticles had selective binding cavities towards CPX. The fast adsorption of CPX on the  $\text{Fe}_3\text{O}_4\text{@MIP}$  nanoparticles also approved that the imprinted nanoparticles showed high mass transfer and better site accessibility for CPX. As a result, the adsorption time of 45 min was selected for further binding experiments.

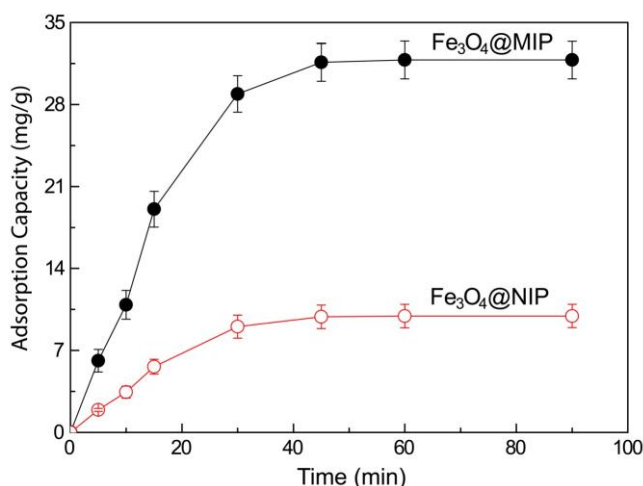


**Figure 5.** Adsorption kinetics of CPX on the  $\text{Fe}_3\text{O}_4\text{@MIP}$  and  $\text{Fe}_3\text{O}_4\text{@NIP}$  nanoparticles (Adsorption conditions: 1.0 mg/mL nanoparticle, 2.2 mg/mL initial concentration of CPX,  $T = 25^\circ\text{C}$ ).

### 3.4. Selectivity of $\text{Fe}_3\text{O}_4\text{@MIP}$ and $\text{Fe}_3\text{O}_4\text{@NIP}$ Nanoparticles

To demonstrate the selectivity of the  $\text{Fe}_3\text{O}_4\text{@MIP}$  and  $\text{Fe}_3\text{O}_4\text{@NIP}$  nanoparticles for CPX, the structural analogues of CPX namely, ciprofloxacin lactate (CPFL) and moxifloxacin (MPX) were selected. The selectivity tests were carried out under the same experimental conditions and the results were displayed in Figure 6. The  $\text{Fe}_3\text{O}_4\text{@MIP}$  nanoparticles had shown much higher adsorption capacity (31.2 mg/g) toward CPX than non-template molecules CPFL (5.2 mg/g) and MPX (4.8 mg/g). In addition, the adsorption capacities of imprinted and non-imprinted nanoparticles for the non-template molecules were similar due to the absence of the specific cavities on the polymer layer. The imprinting factor ( $\alpha = Q_{\text{MIP}}/Q_{\text{NIP}}$  where  $Q_{\text{MIP}}$  and  $Q_{\text{NIP}}$  are the adsorption capacities of CPX for  $\text{Fe}_3\text{O}_4\text{@MIP}$  and  $\text{Fe}_3\text{O}_4\text{@NIP}$  nanoparticles) was determined for the evaluation of the selectivity of the prepared nanoparticles. The imprinting factor values for CPX, CPFL and MPX were calculated as 3.2, 1.48, and 1.37, respectively. The results showed that  $\text{Fe}_3\text{O}_4\text{@MIP}$  nanoparticles were a good adsorbent for enrichment and separation of CPX as a consequence of the formation of specific cavities after polymerization.

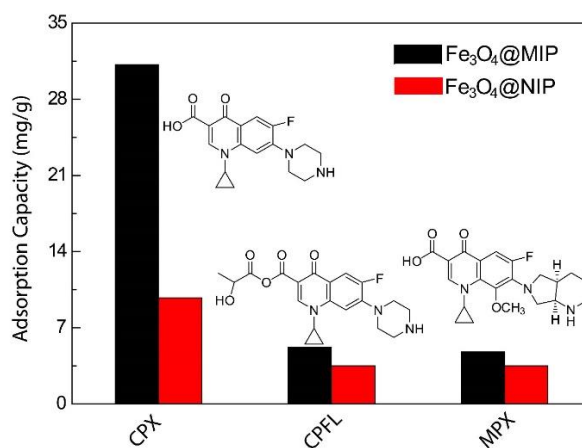


**Fig. 6.** Selectivity of  $Fe_3O_4@MIP$  and  $Fe_3O_4@NIP$  nanoparticles for CPX, CPFL, and MFX (Adsorption conditions: 1.0 mg/mL nanoparticle, 2.2 mg/mL initial concentration of each compound,  $T = 25\text{ }^\circ\text{C}$ ).

### 3.5. Reusability of $Fe_3O_4@MIP$ and $Fe_3O_4@NIP$ Nanoparticles

The reusability of the imprinted magnetic nanoparticles is key parameter for magnetic separation of the interested molecule form complex media. It was thus investigated the stability and reusability of the  $Fe_3O_4@MIP$  nanoparticles by measuring the adsorption capacity in an adsorption-desorption cyclic manner. The  $Fe_3O_4@MIP$  nanoparticles were incubated with CPX for 45 min and the particles were collected by an external magnet. The obtained results were shown in Figure 7. The results indicated that the prepared  $Fe_3O_4@MIP$  nanoparticles had a high stability and good reusability and preserved almost the same recognition abilities for template molecule of CPX even after ten adsorption-desorption cycles.

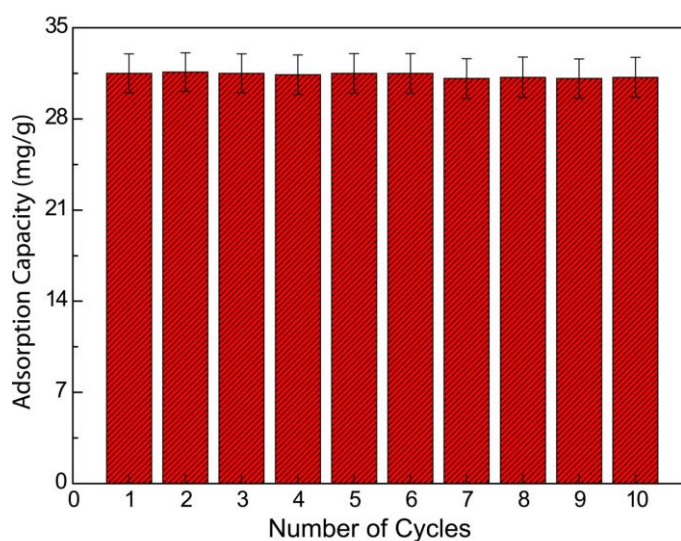


**Figure 7.** Reusability of the  $Fe_3O_4@MIP$  nanoparticles (Adsorption conditions: 1.0 mg/mL nanoparticle, 2.2 mg/mL initial concentration of each compound,  $T = 25\text{ }^\circ\text{C}$ ).

### 3.6. Removal of CPX in Milk Samples

The limit of detection (LOD) and limit of quantification (LOQ) values were calculated for the prepared  $Fe_3O_4@MIP$  nanoparticles in diluted milk samples. The calibration curve was obtained by measuring the average absorbance of known concentrations of CPX ranging from 0.5-100  $\mu\text{g/mL}$ . A good linearity in the range of 0.5-50  $\mu\text{g/mL}$  was obtained. The linear regression equation was  $y = 0.5041x + 0.0436$  with a correlation coefficient 0.9996. The LOD and LOQ values were found to be 0.15  $\mu\text{g/mL}$  and 0.48  $\mu\text{g/mL}$ , respectively.

The risk of the presence of veterinary drug residues, the detection of CPX in milk is of considerable interest since milk is one of the heaviest products in the food industry. The  $Fe_3O_4@MIP$  nanoparticles were evaluated on the capability of removing CPX from milk samples. Before the experiments, milk samples were filtered and diluted with PBS and the diluted samples were spiked with different amounts of CPX. The  $Fe_3O_4@MIP$  nanoparticles were dispersed into spiked samples and incubated for the identical time. The results were tabulated in Table 2. The recovery and relative standard deviation of CPX in milk samples changed from 98.0% to 99.8% and 2.76% to 4.59%, respectively. These results indicated that the  $Fe_3O_4@MIP$  nanoparticles not only had the high binding capacity and affinity for CPX separation in milk but also showed high accuracy and repeatability while employed with real samples.

Concentration of CPX in spiked milk sample ( $\mu\text{g/mL}$ )	Amount found ( $\mu\text{g/mL}$ ) <sup>a</sup>	Recovery (%)	RSD (%) <sup>b</sup>
2.0	1.96 $\pm$ 0.09	98.0	4.59
4.0	3.98 $\pm$ 0.14	99.5	3.52
6.0	5.99 $\pm$ 0.21	99.8	3.50
8.0	7.98 $\pm$ 0.22	99.8	2.76

**Table 2.** Recovery of CPX from spiked milk sample.

<sup>a</sup> Average value from three determinations for each concentration.

<sup>b</sup> Relative standard deviation of band intensity (RSD (%) = (SD/mean) $\times$ 100

To evaluate the interference effect for the detection of CPX by molecularly imprinting method, the diluted milk samples were firstly spiked by CPX and then CPFL, MPX and mixture that contains CPFL and MPX with different molar ratio, respectively. The concentration of CPX was fixed at 2.0  $\mu\text{g/mL}$  for all conditions. The calculated recovery values for CPX were tabulated in Table 3. It can be seen that when CPFL or MPX was present in the CPX solution, the recovery of CPX is 96.9-99.8%. In addition, similar trend was observed for the mixture of CPFL/MPX in the CPX containing milk samples. These results also suggest that  $\text{Fe}_3\text{O}_4\text{@MIP}$  nanoparticles had good size and shape selectivity for CPX in the presence of other structural analogues.

**Table 3.** The interference effect of competitive molecules on determination of CPX in milk<sup>a</sup>.

Molecules	Added	Recovery <sup>b</sup> (%)	Mixture	Added (molar ratio)	Recovery <sup>b</sup> (%)
CPFL	0	99.8	CPFL/MPX	0	100.1
	1	98.9		1	98.5
	5	97.7		5	98.1
	10	96.9		10	96.9
MPX	0	99.9	MPX/CPFL	0	99.8
	1	97.8		1	98.4
	5	96.5		5	97.1
	10	96.3		10	96.8

<sup>a</sup> CPX concentration: 2.0  $\mu\text{g/mL}$ .

<sup>b</sup> Average value from three determinations for each concentration.

### 3.7. Comparison of other methods

To illustrate the advantages of the new magnetic molecularly imprinted nanoparticles as a novel extraction material, the comparative study of proposed method with other reported analytical methodologies for CPX detection and the results are presented in Table 4. It can be seen from the

comparison, lower LOD can be obtained in the present method than other methods so allowing analysis of lower concentration of CPX. The lower LOD can be attributed to not only the presence of the shape memory thin polymer shell layer on the nanoparticle surface but also the high surface area of nanoparticles which can enhance mass transportation.

**Table 4.** Comparison of spectrophotometric methods for CPX determination.

Reagent	Linear range ( $\mu\text{g/mL}$ )	LOD ( $\mu\text{g/mL}$ )	Reference
Cerium (IV)sulphate	1.57-6.28	0.4627	[29]
Eosin and palladium	3-10	0.9112	[30]
Bromocresol green	1-20	0.352	[31]
Cobalt(II) thiocyanate	20-240	0.99	[32]
Bismuth (III) Tetraiodide	5-80	0.40	[33]
$\text{Fe}_3\text{O}_4$ @MIP	0.5-50	0.15	Present Method

#### 4. CONCLUSION

In summary, the surface imprinted magnetic nanoparticles were synthesized using surface-initiated free radical polymerization method for selective separation of CPX. The surface modification of the magnetic nanoparticles was done by using the chemical reaction of methacrylate containing organosilane and the subsequent polymerization of functional monomer in the presence of template molecule CPX. The formed  $\text{Fe}_3\text{O}_4$ @MIP nanoparticles showed superparamagnetic properties allowing the fast separation of the nanoparticles from complex media by an applied external magnet. Moreover, the imprinted nanoparticles had high binding capacity and fast adsorption kinetics. The high selectivity of the prepared nanoparticles suggests that the CPX molecule could be identified from a complex medium such as milk with high recovery and low relative standard deviations. All the results obtained have shown that the developed method is a good alternative to the previously reported analytical methods such as HPLC, voltammetry, immunoassay for CPX determination. The comparison with the spectrophotometric methods for CPX detection in the literature well indicates that the developed method is sensitive and practicable.

#### Acknowledgements

The author thanks to Prof. Dr. Zekiye Suludere for her help in TEM analysis

#### CONFLICTS OF INTEREST

No conflict of interest was declared by the authors.

#### REFERENCES

- [1] Campoli, R.D.M., Monk, P.J., Price, P., Benfield, P., Todd, P., Ward, A., "Ciprofloxacin a review of its antibacterial activity, pharmacokinetic properties and therapeutic use", *Drugs*, 35:373-447 (1988).
- [2] Firsov, A.A., Vostrov, S.N., Shevchenko, A.A., Zinner, S.H., Cornaglia, G., Portnoy, Y.A., "A new approach to in vitro comparisons of antibiotics in dynamic models: equivalent area under the curve/MIC breakpoints and equiefficient doses of trovafloxacin and ciprofloxacin against bacteria of similar susceptibilities", *Antimicrobia. Agents Chemotherapy*, 42:2841-2847 (1998).
- [3] Rao, G. S., Ramesh, S., Ahmad, A. H., Tripathi, H. C., "Pharmacokinetics of enrofloxacin and its metabolite ciprofloxacin in goats given enrofloxacin alone and in combination with probenecid", *The Veterinary Journal*, 163: 85-93 (2002).

- [4] Fang, W. H., Zhou, S., Yu, H. J., Hu, L., Zhou, K., Liang, S., "Pharmacokinetics and tissue distribution of enrofloxacin and its metabolite ciprofloxacin in scylla serrata following oral gavage at two salinities", *Aquaculture*, 272: 180-187 (2007).
- [5] Navalón, A., Blanc, R., Reyes, L., Navas, N., Vilchez, J.L., "Determination of the antibacterial enrofloxacin by differential-pulse adsorptive stripping voltammetry", *Analytica Chimica Acta*, 454:83-91 (2002).
- [6] Gonz'alez, C., Moreno, L., Small, J., Jones, D.G., Bruni, S.F., "A liquid chromatographic method, with fluorometric detection, for the determination of enrofloxacin and ciprofloxacin in plasma and endometrial tissue of mares", *Analytica Chimica Acta*, 560:227-234 (2006).
- [7] Huet, A.C., Charlier, C., Tittlemier, S.A., Singh, G., Benrejeb, S., Delahaut, P., "Simultaneous determination of (fluoro)quinolone antibiotics in kidney, marine products, eggs, and muscle by enzyme-linked immunosorbent assay (ELISA)", *Journal of Agriculture and Food Chemistry*, 54:2822-2827 (2006).
- [8] Cester, C.C., Toutain, P.L., "A comprehensive model for enrofloxacin to ciprofloxacin transformation and disposition in dog", *Journal of Pharmaceutical Sciences*, 86: 1148-1155 (1997).
- [9] Hernández, M., Aguilar, C., Borrull, F., Calull, M., "Determination of ciprofloxacin, enrofloxacin and flumequine in pig plasma samples by capillary isotachopheresis–capillary zone electrophoresis", *Journal of Chromatography B*, 772:163-172 (2002).
- [10] Vlatakis, G., Anderson, L. I., Müller, R., Mosbach, K. "Drug assay using antibody mimics made by molecular imprinting", *Nature*, 361:645-647 (1993).
- [11] Chen, L., Xu, S., Li, J., "Recent advances in molecular imprinting technology: current status, challenges and highlighted applications", *Chemical Society Review*, 40:2922-2942 (2011).
- [12] Chikazumi, S., Taketomi, S., Ukita, M., Mizukami, M., Miyajima, H., Setogawa, M., Kurihara, J., "Physics of magnetic fluids", *Journal of Magnetism and Magnetic Materials*, 65:245-251 (1987).
- [13] Lu, A-H., Schmidt, W., Matoussevitch, N., Bönnemann, H., Spliethoff, B., Tesche, B., Bill, E., Kiefer, W., Schüth, F., "Nanoengineering of a magnetically separable hydrogenation catalyst" *Angewandte Chemie International Edition*, 43:4303-4306 (2004)
- [14] Tsang, S.C., Caps, V., Paraskevas, I., Chadwick, D., Thompsett, D., "Magnetically Separable, Carbon-Supported Nanocatalysts for the Manufacture of Fine Chemicals", *Angewandte Chemie International Edition*, 43:5645-5649 (2004).
- [15] Gupta, A.K., Gupta, M., "Synthesis and surface engineering of iron oxide nanoparticles for biomedical applications", *Biomaterials*, 26:3995-4021 (2005).
- [16] Neveu, S., Bee, A., Robineau, M., Talbot, D., "Size-selective chemical synthesis of tartrate stabilized cobalt ferrite ionic magnetic fluid", *Journal of Colloid and Interface Science*, 255:293-298 (2002).
- [17] Grasset, F., Labhsetwar, N., Li, D., Park, D.C., Saito, N., Haneda, H., Cador, O., Roisnel, T., Mornet, S., Duguet, E., Portier, J., Etourneau, J., "Synthesis and magnetic characterization of zinc ferrite nanoparticles with different environments: powder colloidal solution and zinc ferrite–silica core–shell nanoparticles", *Langmuir*, 18:8209-8216 (2002).
- [18] Sun, S., Zeng, H., "Size-controlled synthesis of magnetite nanoparticles", *Journal of American Chemical Society*, 124:8204–8205 (2002).

- [19] Park, S.J., Kim, S., Lee, S., Khim, Z.G., Char, K., Hyeon, T., "Synthesis and magnetic studies of uniform Iron nanorods and nanospheres Journal of American Chemical Society, 122:8581-8582 (2000).
- [20] Chen, Q., Rondinone, A.J., Chakoumakos, B.C., Zhang, Z.J., "Synthesis of superparamagnetic MgFe<sub>2</sub>O<sub>4</sub> nanoparticles by coprecipitation", Journal of Magnetism and Magnetic Materials, 194:1-7 (1999).
- [21] Ansell, R.J., Mosbach, K., "Magnetic molecularly imprinted polymer beads for drug radioligand binding assay", Analyst, 123: 1611-1616 (1998).
- [22] Tan, C.J., Chua, H.G., Ker, H.K., Tong, Y.W., "Preparation of bovine serum albumin surface-imprinted submicrometer particles with magnetic susceptibility through core-shell miniemulsion polymerization", Analytical Chemistry 80:683-692 (2008).
- [23] Tunturk, H., Sahin, F., Turan, E., "Magnetic nanoparticles coated with different shells or bio recognition high specific binding capacity", Analyst, 139:1093-1100 (2014).
- [24] Bulte, W.M., Cuyper, M., Despres, D., Frank, J.A., "Preparation relaxometry and biokinetics of PEGylated magnetoliposomes as MR contrast agent", Journal of Magnetism and Magnetic Materials, 194:204-209 (1999).
- [25] Smith, G.C., "Evaluation of a simple correction for the hydrocarbon contamination layer in quantitative surface analysis by XPS", Journal of Electron Spectroscopy and Related Phenomena, 148:21-28, (2005).
- [26] Ge, J., Hu, Y., Zhang, T., Yin, Y., "Superparamagnetic composite colloids with anisotropic structures", of American Chemical Society, 129:8974-8975 (2007).
- [27] Umpleby, R.J., Baxter, S.C., Bode, M., Berch, J.K., Shah, R.N., Shimizu, K.D., "Application of the freundlich adsorption isotherm in the characterization of molecularly imprinted polymers original research article", Analytica Chimica Acta, 435:35-42 (2001).
- [28] Adegoke, O.A., Balogun, B.B., "Spectrophotometric determination of some quinolones antibiotics following oxidation with cerium sulphate", International Journal of Pharmaceutical Sciences Review and Research, 4:1-10 (2010).
- [29] El Waliyl, A.F.M., Belal, S.F., Bakry, R.S., "Spectrophotometric and spectrofluorimetric estimation of ciprofloxacin and norfloxacin by ternary complex formation with eosin and palladium(II)" Journal of Pharmaceutical and Biomedical Analysis, 14:561-569 (1996).
- [30] El-Brashy, A.M., Metwally, M.El-S., El-Sepai, F.A., "Spectrophotometric determination of some fluoroquinolone antibacterials through charge-transfer and ion-pair complexation reactions", Bulletin of the Korean Chemical Society, 25:365-372 (2004).
- [31] El-Brashy, A.M., Metwally, M.El-S., El-Sepai, F.A., "Spectrophotometric determination of some fluoroquinolone antibacterials by ion-pair complex formation with cobalt (ii) tetrathiocyanate" Journal of the Chinese Chemical Society, 52:77-84 (2005).
- [32] El-Brashy, A.M., Metwally, M.El-S., El-Sepai, F.A., "Spectrophotometric and atomic absorption spectroscopic determination of some fluoroquinolone antibacterials by ion-pair complex formation with bismuth (iii) tetraiodide" Journal of the Chinese Chemical Society, 52:253-262 (2005).

## SUPPLEMENTARY MATERIAL

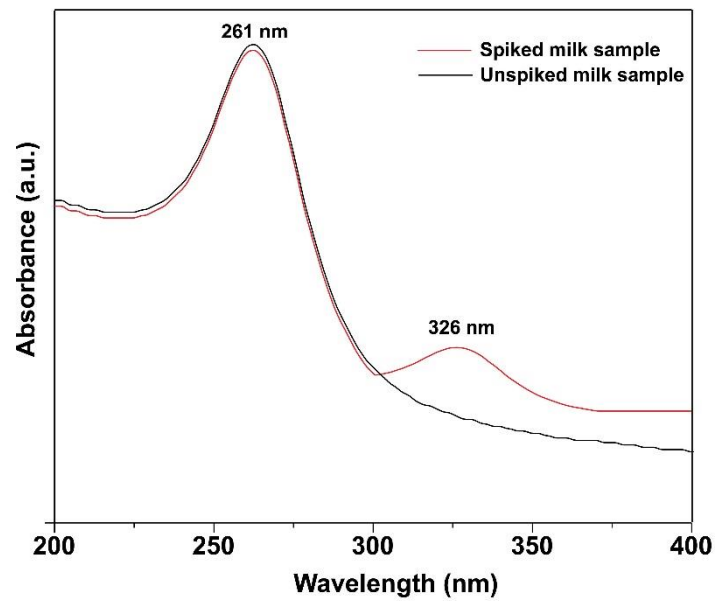


Fig. S1. Uv-vis spectra of unspiked and spiked milk sample (CPX concentration: 8.0  $\mu\text{g/mL}$ )

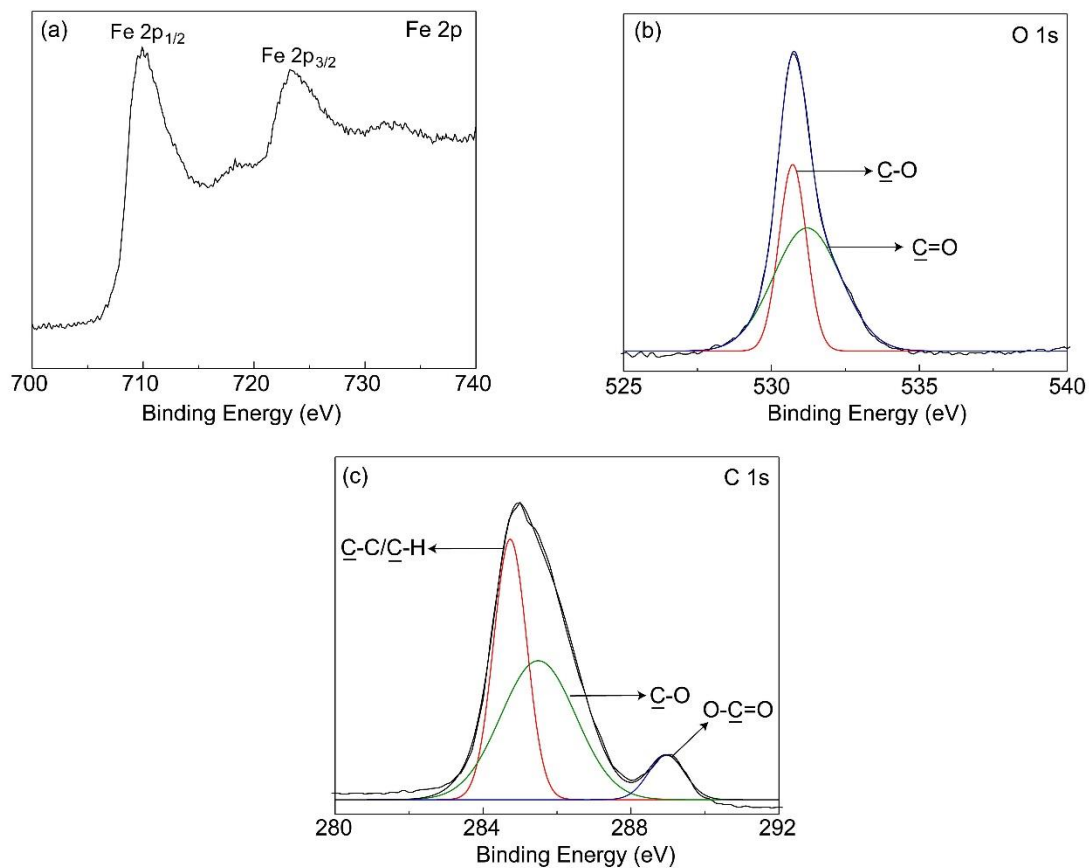


Fig S2. Core-level XPS spectra of Fe<sub>3</sub>O<sub>4</sub>@MPS: (a) Fe 2p, (b) O 1s, (c) C 1s.